Physics-informed Fully Connected and Recurrent Neural Networks for Cardiac Electrophysiology Modelling

Ihsane Olakorede, Iulia Nazarov, Ahmed Qureshi, Shaheim Ogbomo-Harmitt, Oleg Aslanidi

King's College London, London, UK

Abstract

Cardiovascular diseases, the leading cause of death and disability, are often underlined by cardiac arrhythmias. Cardiac electrophysiology models play an increasingly important role in dissecting arrhythmogenic mechanisms and improving treatments, but high computational costs hinder their application. We develop and compare four novel deep learning (DL) models to solve the Fitzhugh-Nagumo (FN) electrophysiology equations efficiently in 0D, 1D and 2D. The training datasets were created using numerical solutions of FN equations. Physics-informed neural network (PINN) was based on the incorporation of FN equations into the Loss function, allowing the optimal combination of training data with physical constraints. Another recurrent NN (RNN) with a mean squared error (MSE) loss function was developed as a baseline. The DL models were evaluated using the MSE score. In 0D and 1D, similar performances were achieved for all DL models, with a typical MSE of 10^{-2}. In 2D, PINN and RNN succeeded in simulating plane and spiral waves with similar MSE of 10^{-2}. Hence, PINNs can provide an efficient tool for cardiac electrophysiology simulations.

1. Introduction

Cardiovascular diseases are a leading cause of morbidity and mortality, accounting for over 30% of all deaths in recent decades. Mechanisms of such diseases are often linked to the occurrence of cardiac arrhythmias – common pathologies caused by disruptions in the generation or propagation of electrical activity in the heart.

Several prominent mechanisms contribute to arrhythmogenesis, such as disruptions in the propagation of cardiac action potentials (APs) by re-entry – a self-sustaining cardiac rhythm abnormality in which the AP propagates in a circuit-like pattern. However, the precise spatio-temporal mechanisms of most arrhythmias are still poorly understood, and the success rate of their treatments remains suboptimal [1]. Computational modelling of cardiac electrophysiology has emerged as a mathematical framework that can incorporate experimental and clinical data, dissect the complex mechanisms of arrhythmias and improve treatments.

AP generation and conduction is mathematically described using ordinary (ODEs) and partial (PDEs) differential equations that are solved numerically. However, the application of such complex models is hindered by the high computational costs of running large-scale simulations for hours and weeks. Hence, the models are generally incompatible with the clinical timescale and impractical to use in the clinic.

Deep learning (DL) models have emerged as an efficient way to solve ODEs/PDEs and overcome the drawbacks from traditional numerical methods. Specifically, Physics-Informed Neural Networks (PINNs) enable combining precise mathematical form of the equations with computational efficiency of DL. This work introduces PINNs as a novel DL tool for simulating cardiac electrophysiology.

2. Methods

Four DL models were developed based on fully connected (FCNNs) and recurrent (RNNs) neural networks, with an additional PINN implementation, to provide solutions to the Fitzhugh-Nagumo (FN) equations. The latter are the simplest equations that can simulate AP propagation, both in normal and arrhythmic conditions. FN equations were first solved numerically in 0D (ODE), 1D and 2D (PDE), and the solutions were then used for training and evaluation of the DL models. The trained DL models were applied for fast simulations of the respective 0D, 1D and 2D electrophysiology patterns.

2.1. Training and Testing Data

The training and test datasets were generated based on numerical solutions of the FN equations using the standard, explicit finite-difference methods with the time step $\Delta t = 0.01$ and the space step $\Delta x = 0.3$. All simulations were performed over T = 100 seconds. For 0D, 1D and 2D DL models, three separate datasets of Tx1, Tx100 and Tx10x10 pixels were generated. Each of the three datasets included a single AP and several periodic APs; the 2D dataset also included a re-entrant spiral wave.

The 0D case corresponds to the evolution of the transmembrane potential in one point of space, mimicking one cardiac cell. The 1D corresponds to

a myocardial cable along which APs propagate. The 2D case describes the propagation of APs over a myocardial tissue; the spiral wave in this case were initiated using the standard cross-field protocol.

To accelerate the training of each network, all datasets were down-sampled 5 times in space in time, with the essential AP properties preserved.

2.2. Neural Networks Architecture

PINNs are a class of neural networks (NNs) that incorporate the underlying physical laws of a given task into the NN's loss function. This enables efficient computations of initial/boundary value problems for ODEs/PDEs with less training data than conventional NNs. Additionally, PINNs make use of automatic differentiation to rewrite the differential equations used to model a system as the minimisation of a residual [2], [3].

Thus, FN equations [4] can be defined as:

$$R(t,\tilde{u},\tilde{n}) = \frac{\partial \tilde{u}}{\partial t} - D\left(\frac{\partial^2 \tilde{u}}{\partial x^2} + \frac{\partial^2 \tilde{u}}{\partial y^2}\right) + k\tilde{u}(\tilde{u} - u_{th})(\tilde{u} - 1) + \tilde{n} + \frac{\partial \tilde{n}}{\partial t} - \varepsilon(g\tilde{u} - \tilde{n}) \quad (1)$$

where $u_{th} = 0.1$ is threshold of the fast sodium current, $\varepsilon = 0.02$ is the control parameter of the relative dynamics between u (voltage) and n (resting variable), and $D = 0.5$ is the diffusion coefficient; other constants were set as $k = 8.0$ and $g = 5.0$.

PINNs are trained to minimise the hybrid loss function, $Loss$, which ensures the learning of known physical laws. $Loss$ accounts for two main terms:

- Agreement with the training data using Mean Squared Error: $MSE_{\tilde{U}} + MSE_{\tilde{N}}$;
- Consistency with the physical laws of the system, residuals: $MSE_{R\_U} + MSE_{R\_N}$; and boundary and initial value conditions: $MSE_{BC} + MSE_{IC}$.

Mathematically, this can be expressed as follows:

$$Loss = MSE_{\tilde{U}+\tilde{N}} + MSE_R + MSE_{BC} + MSE_{IC} \quad (2)$$

$$MSE_{\tilde{U}+\tilde{N}} = \frac{1}{N}\sum_{i=1}^{N}(\tilde{u} - u_{true})^2 + \frac{1}{N}\sum_{i=1}^{N}(\tilde{n} - n_{true})^2 \quad (3)$$

$$MSE_R = MSE[R(t,\tilde{u},\tilde{n})] \quad (4)$$

$$MSE_{IC} = MSE[\tilde{u}(0,x,y), u_{true}(0,x,y)] + MSE[\tilde{n}(0,x,y), n_{true}(0,x,y)] \quad (5)$$

$$MSE_{BC} = MSE[\tilde{u}(t,0,y), u_{true}(t,dx,y)] + MSE[\tilde{u}(t,x_N,y), u_{true}(t,x_{N-1},y)] + MSE[\tilde{u}(t,x,0), u_{true}(t,x,dy)] + MSE[\tilde{u}(t,x,y_N), u_{true}(t,x,y_{N-1})] \quad (6)$$

The custom loss function, $Residual_U$, designed for the surrogate PINN is inspired by the finite-difference methods:

$$Residual_U = \tilde{u}_{t+\Delta t} - \tilde{u}_t - \tilde{u}'\Delta t \quad (7)$$

To evaluate the efficiency of PINNs, traditional FCNNs and RNNs were constructed to compare results obtained using traditional and custom Physics-based loss functions, and to evaluate differences between the DL models. The Physics-based FCNN and surrogate RNN incorporated Equation 2 and the Equation 7, respectively. Figure 1 shows architectures of the three models used in this study, adapted to include the custom loss functions which solves the ODEs and PDEs.

FCNNs take as inputs the time *t* and the spatial coordinates *x* and *y*. The RNNs take as an input an array comprised of time and spatial coordinates.

The number of layers and neurons used is adjusted based on the type of NN. To minimise the $Loss$ and $Residual_U$ functions, adaptive moment estimation (ADAM) optimisation was used with a learning rate of 10^{-4} and $2\text{x}10^{-3}$ for FCNN and RNN, respectively. A mixture of *ReLU* and *tanH* was used as activation functions and Glorot initialisation from a normal distribution was used for all weights.

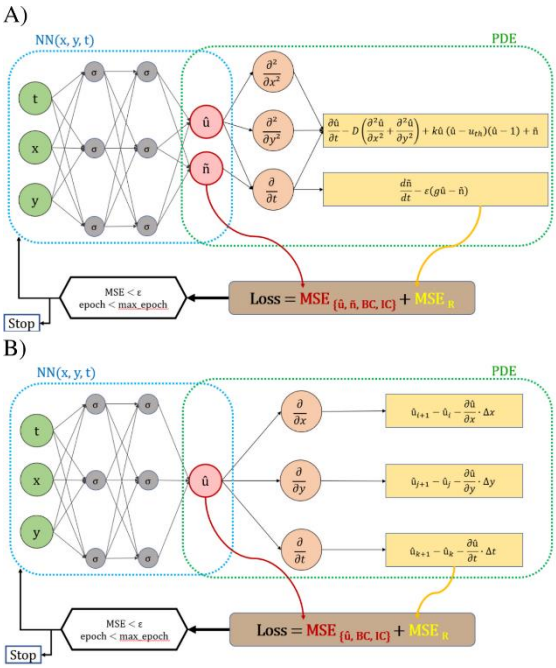

Figure 1. Schematic of PINNs to solve FN equations using A) FCNN and B) RNN. The outputs are differentiated using an automatic differentiation engine to compute the residual. $Loss$ is then computed by summing the residual errors, the boundary, and initial conditions.

The effectiveness and fidelity of the DL models were assessed using the MSE score.

2.3. Training/Testing Split

The test set comes from splitting the full datasets obtained for T = 100s, where 30% of data were kept for testing (time from 50-80s) and the remaining data (0-50s and 80-100s) was used for training.

3. Results

In general, all DL models reproduced AP and wave morphologies in all three dimensions.

Table 1 summarises the model accuracies. The traditional FCNN and RNN were able to reproduce single and repeated APs in all dimensions, as well as a spiral wave in 2D. RNN outperformed all models in simulating single APs in all dimensions.

The FCNN-based PINN model showed high accuracy in reproducing APs in all the examples described. The RNN-based surrogate PINN model had larger errors than regular RNN, but it still produced accurate APs.

	FCNN		RNN	
	MSE	PINN	MSE	PINN
0D	Single AP: < $4x10^{-4}$ Repeated APs: < $4x10^{-2}$			
1D	Single AP: < $7x10^{-4}$ Repeated APs: < $7x10^{-3}$			
2D Plane	4.69 $x10^{-4}$	3.85 $x10^{-3}$	9.27 $x10^{-4}$	3.85 $x10^{-3}$
2D Spiral	1.14 $x10^{-3}$	4.20 $x10^{-3}$	1.87 $x10^{-3}$	2.69 $x10^{-3}$

Table 1: MSE scores for all DL models. Lower scores were seen for a single AP compared to the case of repeated APs in 0D and 1D, as well as for the plane waves compared to spiral waves in 2D.

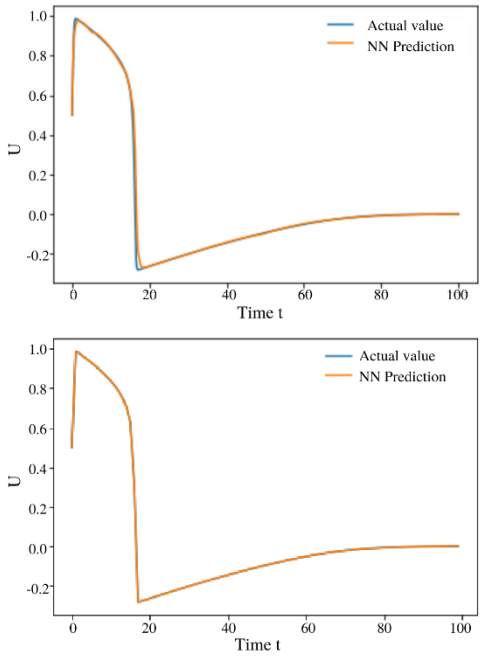

Figure 2. Approximation of a single AP solution of FN equations over 100 s in 0D using the PINN *Loss* function for the FCNN *(top)* and RNN *(bottom)* models, with blue representing the ground truth solution and orange the NNs predictions.

Figures 2 and 3 illustrate the performance comparison of the two PINN implementations in 0D and 1D for single APs. RNN-based surrogate PINN outperformed FCNN-based PINN in both cases.

The 2D spiral wave propagation predicted by the DL models is shown in Figure 4. The wavefront for the traditional FCNN and RNN is compared to the same spiral wave predicted using the PINN. The traditional RNN errors were larger at the borders of the 2D tissue, in contrast to FCNN results, where errors occurred at the wavefront (Figure 4, top panels). The Physics-based FCNN simulates the spiral wave, while the RNN surrogate PINN produced a more accurate simulation (Table 1; Figure 4, bottom panels). These results are due to the hypermeandering of the spiral wave [5], which is difficult to predict without accounting for the spiral's movement over a long period of time.

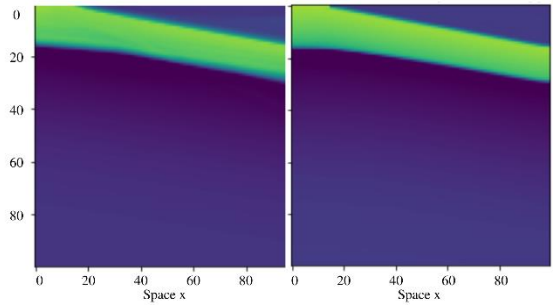

Figure 3. Space-time plots of AP propagation along a 1D cable for both the PINN models, FCNN (left) and RNN (right). The cable boundaries are the main source of errors. Yellow/green and blue indicate AP and resting potential, respectively.

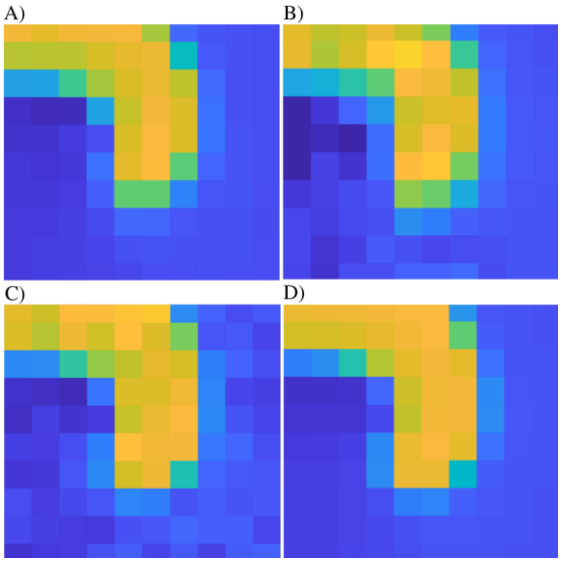

Figure 4. Prediction of a 2D spiral wave in a down-sampled 20x20 tissue at t = 99s, using the traditional FCNN (A) and RNN (B), and using the PINN *Loss* for the FCNN (C). The ground truth is shown for comparison (D). Yellow/green indicates depolarised regions, blue corresponds to resting regions.

4. Discussion

This study demonstrates the potential of DL, and in particular PINNs, for efficient simulations of cardiac electrophysiology. The training of PINNs was performed using a comparatively simple FN model in 0D, 1D and 2D scenarios. The main results of this study are: i) reproducing a single AP in 0D (single cell), 1D (cable) and 2D (tissue); ii) simulating repeated APs in 0D and 1D; iii) simulating a spiral wave in 2D tissue; iv) integrating Physics-informed loss functions; and v) comparing DL models for the same scenarios. All models reproduced the ground truth solutions of the FN equations.

Few studies have considered the application of PINNs to solve differential equations for cardiac electrophysiology. Martin et al. [6] have recently applied DL for simulations of the Aliev-Panfilov model in 2D for planar, circular, and spiral waves, with/without a region of heterogeneity. Kashtanova et al. [7] extended an earlier Ayed et al. [8] model to simulate the Mitchell-Schaffer model in 2D, also including region of heterogeneity (scars).

Validation and evaluation of the findings was achieved by comparing the DL predictions to the ground truth and to the previous studies. Specifically, the evaluation was accomplished by comparing the accuracy of DL predictions to the results obtained in previous studies of 2D planar and spiral wave. Ayed et al. obtained MSE of $5x10^{-3}$ for a planar wave with their CNN-based PINN, which was outperformed by our models. Martin et al. acquired a minimum MSE of $9x10^{-4}$ for both planar and spiral waves, which was close to our results.

Thus, our study evaluated the performance of PINNs for cardiac electrophysiology modelling and showed their superiority over conventional NNs. Moreover, we also showed how RNN's temporal dynamic behaviour facilitates it in predicting complex patterns like spiral waves with good accuracy. Future work should focus on extending our surrogate RNN loss function with a physical component to obtain more accurate predictions.

5. Conclusion

This research shows growing potential of PINNs that utilise physical information to solve ODEs and PDEs for biomedical applications. The FN equations describing AP propagation in 0D, 1D and 2D can be solved using traditional NNs and PINNs. Both types of networks achieve sensibly accurate predictions. PINNs combine the speed and powerful function approximation ability of NNs and the physical information contained in the equations. Hence, PINNs can provide an efficient computational tool for cardiac electrophysiology simulations.

Acknowledgments

This work was supported by funding from the Medical Research Council [MR/N013700/1], the British Heart Foundation [PG/15/8/31130], and the Wellcome/EPSRC Centre for Medical Engineering [WT 203148/Z/16/Z].

References

[1] H. Calkins *et al.*, "2012 HRS/EHRA/ECAS Expert Consensus Statement on Catheter and Surgical Ablation of Atrial Fibrillation: Recommendations for Patient Selection, Procedural Techniques, Patient Management and Follow-up, Definitions, Endpoints, and Research Trial Design," *Heart Rhythm*, vol. 9, no. 4, pp. 632-696. e21, Apr. 2012

[2] M. Raissi, P. Perdikaris, and G. E. Karniadakis, "Physics-informed neural networks: A deep learning framework for solving forward and inverse problems involving nonlinear partial differential equations," *Journal of Computational Physics*, vol. 378, pp. 686–707, Feb. 2019

[3] I. E. Lagaris, A. Likas, and D. I. Fotiadis, "Artificial neural networks for solving ordinary and partial differential equations," *IEEE Transactions on Neural Networks*, vol. 9, no. 5, pp. 987–1000, 1998.

[4] O. A. Mornev, O. V. Aslanidi, R. R. Aliev, and L. M. Chaĭlakhian, "Soliton-like regime in the Fitzhugh-Nagumo equations: reflection of colliding excitation pulses," *Dokl Akad Nauk*, vol. 347, no. 1, pp. 123–5, Mar. 1996.

[5] A. Roy *et al*., "Identifying locations of re-entrant drivers from patient-specific distribution of fibrosis in the left atrium," *PLoS Computational Biology*., vol. 16(9), e1008086, Sep. 2020.

[6] C. Herrero Martin *et al.*, "EP-PINNs: Cardiac Electrophysiology Characterisation Using Physics-Informed Neural Networks," *Frontiers in Cardiovascular Medicine*, vol. 8, Feb. 2022.

[7] V. Kashtanova, I. Ayed, N. Cedilnik, P. Gallinari, and M. Sermesant, "EP-Net 2.0: Out-of-Domain Generalisation for Deep Learning Models of Cardiac Electrophysiology," *11th International Conference on Functional Imaging & Modeling of the Hearth*, pp. 482–492, Jun. 2021.

[8] I. Ayed, N. Cedalnik, P. Gallinari, and M. Sermesant, "EP-Net: Learning Cardiac Electrophysiology Models for Physiology-based Constraints in Data-Driven Predictions," *10th International Conference on Functional Imaging & Modeling of the Hearth*, pp. 55–63, Jun. 2019.

Address for correspondence:

Shaheim Ogbomo-Harmitt
School of Biomedical Engineering and Imaging Sciences, King's College London, 3rd Floor Lambeth Wing, St Thomas' Hospital, London SE1 7EH, UK
shaheim.ogbomo-harmitt@kcl.ac.uk